Measurement and Modeling of Alloy-Spinel-Corundum Equilibrium in the Ni-Mn-Al-O System at 1873 K

S. SHASHIDHARA PANDIT and K.T. JACOB

The oxygen content of liquid Ni-Mn alloy equilibrated with spinel solid solution, $(Ni, Mn)O \cdot (1 + x)Al_2O_3$, and α-Al_2O_3 has been measured by suction sampling and inert gas fusion analysis. The corresponding oxygen potential of the three-phase system has been determined with a solid state cell incorporating $(Y_2O_3)ThO_2$ as the solid electrolyte and $Cr + Cr_2O_3$ as the reference electrode. The equilibrium composition of the spinel phase formed at the interface of the alloy and alumina crucible was obtained using EPMA. The experimental data are compared with a thermodynamic model based on the free energies of formation of end-member spinels, free energy of solution of oxygen in liquid nickel, interaction parameters, and the activities in liquid Ni-Mn alloy and spinel solid solution. Mixing properties of the spinel solid solution are derived from a cation distribution model. The computational results agree with the experimental data on oxygen concentration, potential, and composition of the spinel phase.

I. INTRODUCTION

THE ability to compute the deoxidation equilibria in multicomponent systems of industrial importance is useful for process optimization. As part of a larger program on validating computational codes, studies have been carried out on Fe-Mn-Al-O,[1] Co-Mn-Al-O,[2] and Fe-Ni-Al-O[3] systems. This study focuses on the Ni-Mn-Al-O system in which the cation distribution in the spinel solid solution changes from nearly inverse to normal with increase in manganese concentration.

When aluminum is used as the deoxidant for Ni-Mn alloys, the deoxidation product is alumina at low oxygen or high aluminum concentration. At lower concentrations of the deoxidant, spinel solid solution, $(Ni, Mn)O \cdot (1 + x)Al_2O_3$, forms. The Ni/Mn concentration ratio in the spinel phase is a function of the alloy composition. In this study, the critical oxygen concentration and potential for the transition from alumina to spinel have been measured as a function of alloy composition (Ni/Mn ratio) at 1873 K. The composition of the spinel solid solution was measured using Electron Probe Microanalysis (EPMA). The experimental results are compared with computations based on a thermodynamic model. Data on activities in Ni-Mn alloys,[4,5] free energies of formation of $NiO \cdot (1 + x)Al_2O_3$ and $MnO \cdot (1 + x)Al_2O_3$,[6,7] free energy of solution of oxygen in liquid nickel,[6] and interaction parameters[8,9] are taken from the literature. The composition dependence of activities of spinel solid solutions was generated by a structural model[10] involving exchange of cations between tetrahedral and octahedral sites.

II. EXPERIMENTAL

The apparatus used in this study was identical to that used earlier.[2] Approximately 50 g of Ni-Mn alloy and 5 g of an equimolar mixture of $NiAl_2O_4$ (or $MnAl_2O_4$) and α-alumina were taken in an alumina crucible held in the even-temperature zone of the vertical molybdenum wound resistance furnace under flowing inert gas. An yttria-stabilized thoria tube containing a mixture of $Cr + Cr_2O_3$ in the molar ratio of $3:1$ was used for oxygen potential measurement. Electrical contact to the $Cr + Cr_2O_3$ reference mixture was made by Pt-5 pct Rh wire. The electrical contact to the alloy was effected through a short tungsten rod held in an alumina tube and connected to Pt-5 pct Rh wire. Both the solid electrolyte and the tungsten rod were generally held above the melt during equilibration and were inserted into the alloy only for short periods for emf measurements. Induced emf on the electrode leads was eliminated by placing an earthed molybdenum shield between the furnace and working tubes. Suction samples from the melt were taken with silica tubes flushed with argon gas. The temperature of the melt was controlled to ± 2 K and measured by a Pt-5 pct Rh/Pt-20 pct Rh thermocouple.

In preliminary studies variation of the oxygen concentration and emf were monitored as a function of time. It was found that equilibrium was attained in 2 to 2.5 hours. In subsequent experiments, the melt was held at 1873 K for 3 hours before taking suction samples or emf measurements. The emf was measured with a digital voltmeter with an input impedance greater than 10^{12} Ω. The emf became steady in ~ 60 seconds after immersion of the tube and remained constant for up to 600 seconds. There was a gradual decrease after this period. The decay of the emf could be partially arrested by vibrating the thoria tube. This suggests the build-up of concentration polarization in the melt adjacent to the thoria tube, caused by either physical or electrochemical permeability of the electrolyte to oxygen. The concentration polarization at the reference electrode due to the semipermeability flux of oxygen through the electrolyte was minimized by taking large excess of Cr in finely divided form. Addition of small amounts (~ 0.05 g) of α-Al_2O_3 to the melt did not alter the emf, confirming that the alloy was in equilibrium not only with the aluminate but also with α-Al_2O_3. The thoria tube was mildly attacked by both the alloy melt and the $Cr + Cr_2O_3$ reference electrode.

Analysis of the alloy at the end of some typical experiments indicated that the tungsten pick-up was less than 0.1 wt pct. Visual examination of the melt during experiments and the solidified ingot and the crucible after experi-

S. SHASHIDHARA PANDIT, Scientific Assistant and Candidate for Ph.D., and K.T. JACOB, Professor and Chairman, are with the Department of Metallurgy, Indian Institute of Science, Bangalore 560 012, India.
Manuscript submitted August 10, 1987.

ments indicated that the aluminate phase was mainly present at the surface of the melt and the metal/crucible interface. After each experiment, the crucible was sectioned and the composition of the aluminate phase on the inner side of the crucible wall was determined by electronprobe microanalysis using pure MnO, NiO, and α-Al$_2$O$_3$ as standards. The manganese and oxygen contents of the alloy samples were determined by chemical analysis. The oxygen concentration was measured by an inert gas fusion technique using a LECO gas analyzer (model TC-236).

III. RESULTS

The experimental data on emf, oxygen content, and equilibrium composition of the alloy and the spinel solid solution corresponding to the three-phase equilibrium are summarized in Table I. The increase in the manganese content of the spinel solid solution with increase in mole fraction of manganese in the alloy is shown in Figure 1. The oxygen
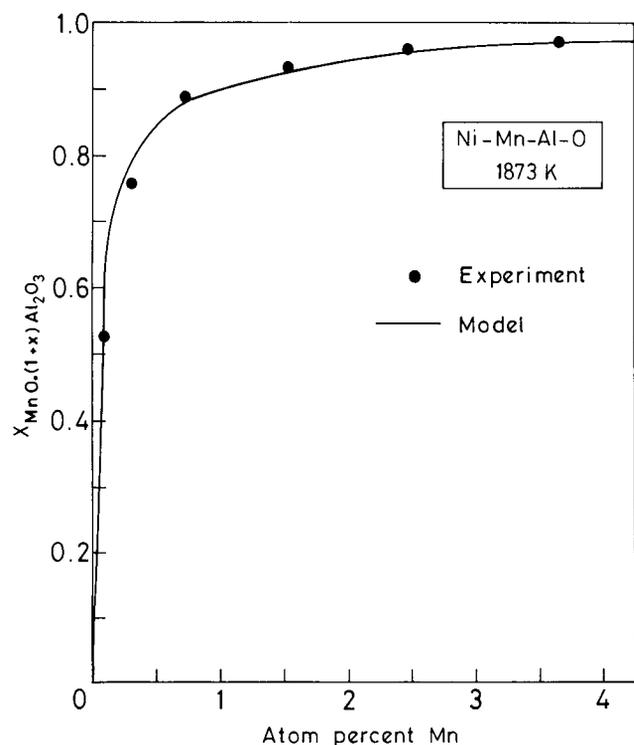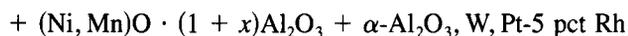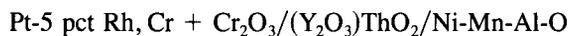

Fig. 1 — Variation of the equilibrium composition of the spinel solid solution with alloy composition at 1873 K.

potential corresponding to the three-phase equilibrium between alloy, spinel solid solution, and α-alumina can be computed from the emf of the solid state cell:

Pt-5 pct Rh, Cr + Cr$_2$O$_3$/(Y$_2$O$_3$)ThO$_2$/Ni-Mn-Al-O
+ (Ni, Mn)O · (1 + x)Al$_2$O$_3$ + α-Al$_2$O$_3$, W, Pt-5 pct Rh

$$4FE = \Delta\mu_{O_2} - \Delta\mu_{O_2(Cr+Cr_2O_3)} \quad [1]$$

where E is the emf, F is the Faraday constant, $\Delta\mu_{O_2}$ is the oxygen potential corresponding to the three-phase equilibrium defined by either of the following reactions:[6,7]

$$\underline{Ni}(l) + \frac{1}{2}O_2(g) +$$

$$(1 + x)Al_2O_3(\alpha) \rightarrow [NiO \cdot (1 + x)Al_2O_3](sp) \quad [2]$$

$$\Delta G_2^\circ = -259,410 + 84.4T \quad (\pm 350) \text{ J mol}^{-1} \quad [3]$$

$$\underline{Mn}(l) + \frac{1}{2}O_2(g) +$$

$$(1 + x)Al_2O_3(\alpha) \rightarrow [MnO \cdot (1 + x)Al_2O_3](sp) \quad [4]$$

$$\Delta G_4^\circ = -444,460 + 94.27T \quad (\pm 1500) \text{ J mol}^{-1} \quad [5]$$

where components in the liquid are underlined and the components in the spinel solid solution are enclosed within square brackets. The oxygen potential of the Cr + Cr$_2$O$_3$ reference electrode is given by:[11,12]

$$\Delta\mu_{O_2(Cr+Cr_2O_3)} = -743,960 + 166.9T \quad (\pm 600) \text{ J mol}^{-1} \quad [6]$$

The decrease of the oxygen potential with manganese concentration is shown as data points in Figure 2. The variation of the equilibrium oxygen content of the alloy with composition at 1873 K is shown in Figure 3. There is a steep decrease in the equilibrium oxygen content of the alloy up to ~0.3 at. pct manganese. The oxygen content is not very sensitive to manganese concentration between 1 and 4 at. pct.

IV. MODEL

The parameters characterizing the three-phase equilibrium between the alloy, spinel, and α-alumina can be computed from the basic thermodynamic data. Information on activities in the alloy,[4,5] Gibbs energies of formation of end-member spinel compounds,[6,7] free energy of solution of oxygen in liquid nickel,[6] and interaction parameters[8,9] are available in the literature. The missing information re-

Table I. Equilibrium Compositions of the Alloy and Spinel Solid Solution, Emf, and Oxygen Potential for the Three-Phase System at 1873 K
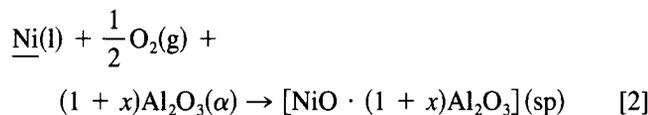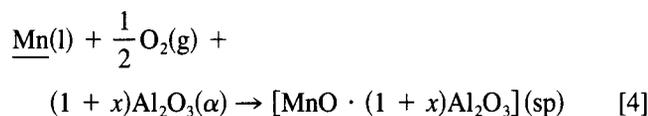
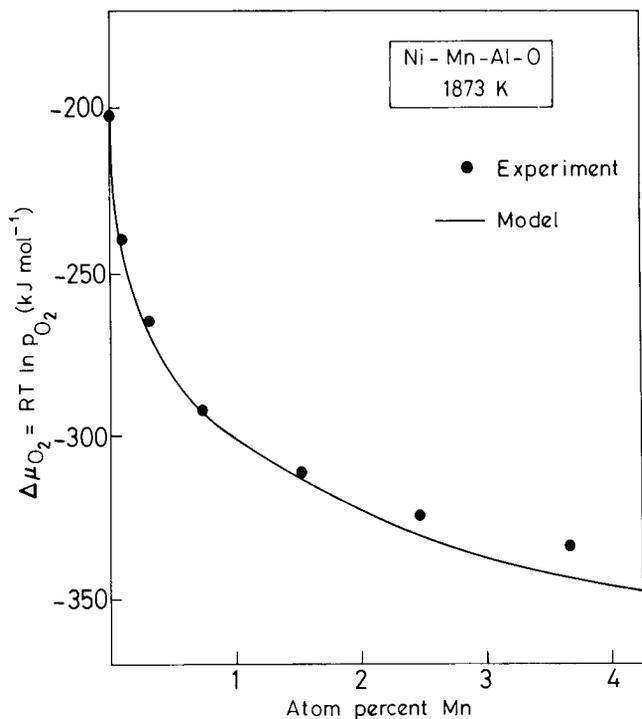| Composition of the Alloy		Composition of the Spinel Solid Solution	Emf, mV	$\Delta\mu_{O_2}$,	
At. Pct Mn	At. Pct O	At. Pct MnO · (1 + x)Al$_2$O$_3$	($\pm$1)	kJ mol^{-1}	log γ_O
0.000	0.401	0.0	593	-202.44	-2.426
0.104	0.124	52.4	497	-239.62	-2.435
0.297	0.055	76.0	431	-265.18	-2.438
0.740	0.027	89.2	361	-292.04	-2.504
1.520	0.016	93.0	310	-311.60	-2.549
2.460	0.012	96.1	280	-323.44	-2.589
3.670	0.010	97.3	253	-333.66	-2.653

Fig. 2—Dependence of the oxygen potential of the three-phase alloy + spinel + corundum system on alloy composition at 1873 K.
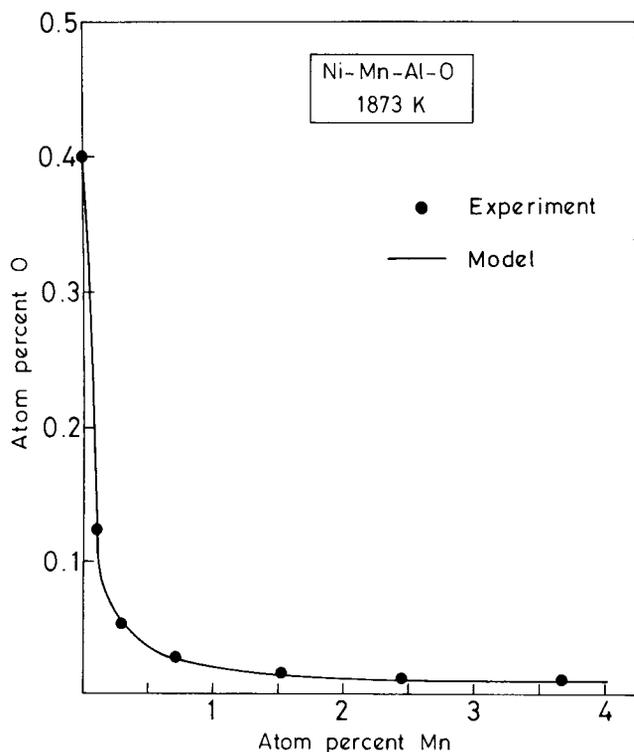

Fig. 3—Variation of the oxygen content of the alloy corresponding to the three-phase equilibrium with manganese concentration of the alloy at 1873 K.

garding activity-composition relationship in the spinel solid solution is computed using a cation distribution model.[10] The distribution of the three cations Ni^{2+}, Mn^{2+}, and Al^{3+} between the tetrahedral and octahedral interstitial sites in an approximately close-packed lattice of oxygen ions is

determined by the octahedral site preference energies of the cations. The values of the octahedral site preference energies are -86.2 kJ mol^{-1} for Ni^{2+}, 0 kJ mol^{-1} for Mn^{2+}, and -77.82 kJ mol^{-1} for Al^{3+} ions.[13] Thus pure nickel aluminate is an inverse spinel and manganese aluminate is a normal spinel at low temperatures. At higher temperatures, the cations exchange positions as a consequence of the resulting increase in entropy. The cation exchange can be represented by:

$$[Ni^{2+}] + (Al^{3+}) \rightarrow (Ni^{2+}) + [Al^{3+}] \qquad [7]$$

$$(Mn^{2+}) + [Al^{3+}] \rightarrow [Mn^{2+}] + (Al^{3+}) \qquad [8]$$
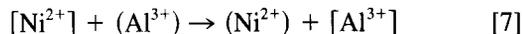
where ( ) indicates tetrahedral site and [ ] the octahedral site. The extent of mixing depends on the exchange enthalpy, ΔH^{ex}, which is the difference in the octahedral site preference energies of the two competing cations. The standard enthalpy change for the exchange reactions [7] and [8], which are balanced both with respect to ions and sites, is negligible. Assuming ideal entropy of mixing on each cation sublattice, one obtains:

$$\Delta H_7^{ex} = -RT \ln \frac{(N_{Ni^{2+}})[N_{Al^{3+}}]}{[N_{Ni^{2+}}](N_{Al^{3+}})}$$

$$= -8,370 \text{ J mol}^{-1} \qquad [9]$$

$$\Delta H_8^{ex} = -RT \ln \frac{[N_{Mn^{2+}}](N_{Al^{3+}})}{(N_{Mn^{2+}})[N_{Al^{3+}}]}$$

$$= 77,820 \text{ J mol}^{-1} \qquad [10]$$

The associated mass and site balance equations for the cations are:

$$(N_{Ni^{2+}}) + 2[N_{Ni^{2+}}] = X_{NiAl_2O_4} \qquad [11]$$

$$(N_{Mn^{2+}}) + 2[N_{Mn^{2+}}] = X_{MnAl_2O_4} = 1 - X_{NiAl_2O_4} \qquad [12]$$

$$(N_{Ni^{2+}}) + (N_{Mn^{2+}}) + (N_{Al^{3+}}) = 1 \qquad [13]$$

$$[N_{Ni^{2+}}] + [N_{Mn^{2+}}] + [N_{Al^{3+}}] = 1 \qquad [14]$$

where N_i represents the ionic fraction of the cation i on a specified site and X represents the mole fraction of the spinel component. Using Eqs. [9] to [14], the cation distribution can be calculated for the pure spinels or spinel solid solutions. The results are shown in Figure 4. The activities in the spinel solid solution can be calculated from the cation distribution using the expressions,

$$a_{NiAl_2O_4} = \frac{[N_{Ni^{2+}}](N_{Al^{3+}})[N_{Al^{3+}}]}{[N_{Ni^{2+}}^o](N_{Al^{3+}}^o)[N_{Al^{3+}}^o]} \qquad [15]$$

and

$$a_{MnAl_2O_4} = \frac{(N_{Mn^{2+}})[N_{Al^{3+}}]^2}{(N_{Mn^{2+}}^o)[N_{Al^{3+}}^o]^2} \qquad [16]$$

where N_i^o represents the ionic fraction of cation i in the end-member spinel. The computed activity-composition relationship at 1873 K is shown in Figure 5. The activities of both components of the spinel solid solution show negative deviations from Raoult's Law.

The composition of the spinel phase in equilibrium with different alloys can be computed from the standard free energy change for the reaction:[6,7]
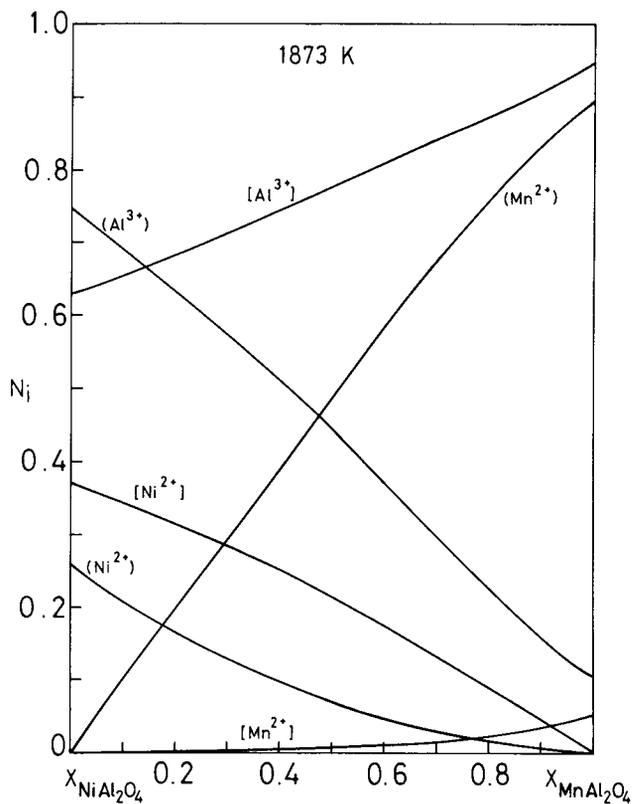
Fig. 4—Computed cation distribution in $(Ni, Mn)Al_2O_4$ spinel solid solution at 1873 K.
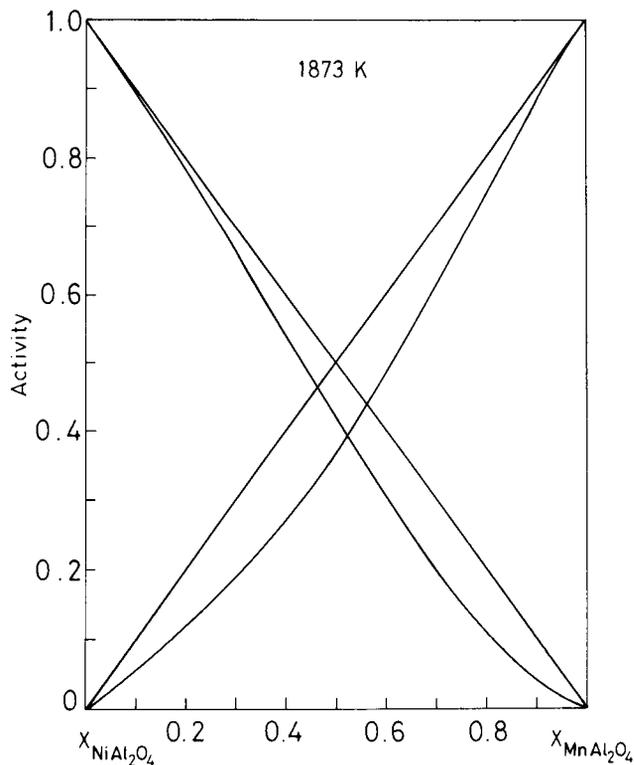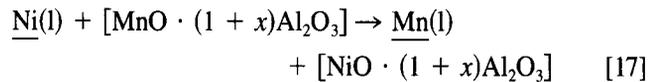

Fig. 5—Activities of components in the spinel solid solution $NiAl_2O_4$-$MnAl_2O_4$ at 1873 K computed from cation distribution.

$$\underline{Ni}(l) + [MnO \cdot (1 + x)Al_2O_3] \rightarrow \underline{Mn}(l)$$
$$+ [NiO \cdot (1 + x)Al_2O_3] \qquad [17]$$

$$\Delta G^{\circ}_{17} = -RT \ln \frac{a_{Mn}a_{NiO \cdot (1+x)Al_2O_3}}{a_{Ni}a_{MnO \cdot (1+x)Al_2O_3}}$$

$$= -RT \ln \frac{X_{Mn}\gamma_{Mn}a_{NiO \cdot (1+x)Al_2O_3}}{X_{Ni}\gamma_{Ni}a_{MnO \cdot (1+x)Al_2O_3}}$$

$$= 185,050 - 9.87T \qquad J \ mol^{-1} \qquad [18]$$

Activities in Ni-Mn alloys reported by Jacob[4] at 1683 K conform to a subregular model. Enthalpies of mixing of liquid Ni-Mn alloys at 1773 K have been determined calorimetrically by Batalin et al.[5] Their data can be represented in a subregular format:

$$\Delta H^M = X_{Ni}X_{Mn}[-39,290X_{Mn} - 56,330X_{Ni}] \qquad J \ mol^{-1}$$
$$[19]$$

The activity coefficients at 1873 K can be obtained by combining the free energy measurements at 1683 K with calorimetric data:

$$\log \gamma_{Mn} = -0.4275X^2_{Ni} - 0.9288X^3_{Ni} \qquad [20]$$

$$\log \gamma_{Ni} = -1.8208X^2_{Mn} + 0.9288X^3_{Mn} \qquad [21]$$

The ratio of the activities in the spinel solid solution in equilibrium with the alloy can be calculated from Eq. [18] as a function of alloy composition. The actual composition of the spinel solid solution can be computed from the activity-composition relationship shown in Figure 5. The computed compositions of the spinel solid solution are in good agreement with the experimental results as shown in Figure 1.

The equilibrium oxygen potential of the three-phase system can be computed using either reaction [2] or [4]. The variation of the oxygen potential with alloy composition is in fair agreement with experimental data as shown in Figure 2. From the known oxygen potential over the three-phase system, the oxygen concentration in the alloy can be computed using the free energy of solution of gaseous oxygen in liquid nickel[6] and the interaction parameters.[8,9]

$$\frac{1}{2} O_2(g) \rightarrow \underline{O}_{Ni} \qquad [22]$$

$$\Delta G^{\circ}_{22} = -72,930 - 7.11T \qquad J \ g. \ at.^{-1} \qquad [23]$$

$$\log f^O_O = \left(-\frac{500}{T} + 0.216\right) at. \ pct \ O \qquad [24]$$

$$\varepsilon^{Mn}_O = \frac{\partial \ln f^{Mn}_O}{\partial X_{Mn}} = -15.6 \qquad [25]$$

The equilibrium constant for the reaction [22] is

$$K_{22} = \frac{at. \ pct \ Of^O_O f^{Mn}_O}{p^{1/2}_{O_2}} \qquad [26]$$

Combining Eqs. [23] to [26] one gets,

(at. pct O) exp(−0.1173 at. pct O)

$$= 254.31p^{1/2}_{O_2}/exp(-15.6X_{Mn}) \qquad [27]$$
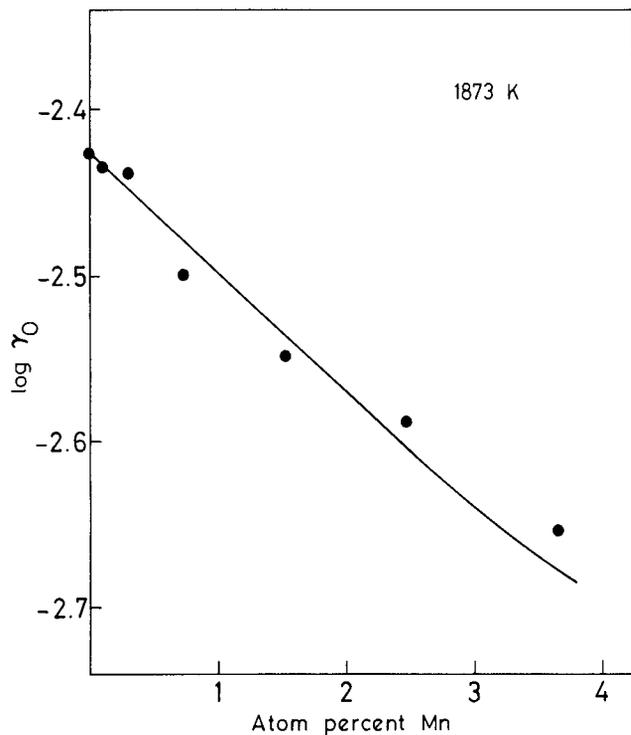
Fig. 6—Variation of log γ_O with manganese concentration at 1873 K.

V. CONCLUSIONS

The experimental results on the equilibrium oxygen concentration and potential and the composition of the spinel phase corresponding to the three-phase equilibrium in the Ni-Mn-Al-O system at 1873 K are in good agreement with model calculations based on the thermodynamic data reported in the literature. The present experimental results confirm the value for oxygen-manganese interaction ($\varepsilon_O^{Mn} = -15.6$) given by Janke and Fischer.[9] The use of a cation distribution model for deriving activities in spinel solid solution is validated by experimental results obtained in this study. It is worthwhile to extend these model computations to higher order systems of practical interest, with spot measurements at large intervals of composition for verification.

The oxygen concentration obtained by solving Eq. [27] using an iterative procedure is plotted as a function of alloy composition in Figure 3 as a solid line. The computed values match well with the experimental data, validating the model and the data used in the computation.

The value of $\varepsilon_O^{Mn} = -15.6$ used in this computation was taken from Janke and Fischer.[9] It differs substantially from the value of -97 suggested in the compilation of Sigworth et al.[8] An approximate value of the interaction parameter can be derived from the oxygen potentials and concentrations measured in this study. The variation of the logarithm of the activity coefficient of oxygen [$\gamma_O = p_{O_2}^{1/2}/(\text{at. pct O})$] with manganese concentration is plotted in Figure 6. From the slope of the curve a value of -17 (± 2) is obtained for ε_O^{Mn}, in good agreement with the value suggested by Janke and Fischer.[9]

REFERENCES

1. S. S. Pandit and K.T. Jacob: *Arch. Eisenhüttenw.*, 1987, vol. 58, pp. 105-10.
2. K. T. Jacob and S. S. Pandit: *Z. Metallkde.*, 1987, vol. 78, pp. 652-56.
3. K. T. Jacob and S. S. Pandit: *Trans. ISIJ*, 1988, vol. 28, in press.
4. K. T. Jacob: *Metall. Trans. B*, 1982, vol. 13B, pp. 283-85.
5. G. I. Batalin, V. A. Stukalo, N.Ya. Neshimenko, and N. V. Patselii: *Russ. J. Phys. Chem.*, 1981, vol. 55, pp. 1395-97.
6. K. T. Jacob: *Metall. Trans. B*, 1986, vol. 17B, pp. 763-70.
7. K. T. Jacob: *Canad. Met. Quart.*, 1981, vol. 20, pp. 89-92.
8. G. K. Sigworth, J. F. Elliott, G. Vaughan, and G. H. Geiger: *Trans. Met. Soc. C.I.M.*, 1977, pp. 104-10.
9. D. Janke and W. A. Fischer: *Arch. Eisenhüttenw.*, 1975, vol. 46, pp. 297-302.
10. K. T. Jacob and C. B. Alcock: *J. Solid State Chem.*, 1977, vol. 20, pp. 79-88.
11. K. T. Jacob: *J. Electrochem. Soc.*, 1977, vol. 124, pp. 1827-31.
12. K. T. Jacob and B. V. Kumar: *Z. Metallkde.*, 1986, vol. 77, pp. 207-11.
13. J. D. Dunitz and L. E. Orgel: *J. Phys. Chem. Solids*, 1957, vol. 3, pp. 318-23.